 The archival version of this work was published in *Electrochemical and Solid-State Letters*, 3 (6) 268-270 (2000). doi:10.1149/1.1391121

Anisotropy of Localized Corrosion in AA2024-T3

Weilong Zhang[*] and G. S. Frankel[,z]**

Department of Materials Science and Engineering, The Fontana Corrosion Center, The Ohio State University, Columbus, Ohio 43210, USA

The foil penetration technique and metallographic cross sections were used to study the kinetics and morphology of localized corrosion in AA2024-T3 in different orientations relative to the rolling direction. The foil penetration technique measures the time for the fastest-growing localized corrosion site (pit, crevice, or intergranular attack) to penetrate foils of various thickness. The growth kinetics of localized corrosion in AA2024-T3 exhibited a strong anisotropy. Growth in the short transverse direction (through-thickness direction of a rolled plate) was found to be much slower than that in either the longitudinal or long transverse direction. The effect of microstructure occurred because pits that initiated on the surface often transformed into intergranular corrosion. The anisotropy of the microstructure in this alloy results in a vast difference in intergranular path length per nominal thickness for various orientations. However, the pitting potential of AA2024-T3 was found to be almost independent of sample orientation relative to the rolling direction.

There is increasing scientific and practical interest in quantitatively measuring localized corrosion growth rates in Al alloys since most high strength Al alloys widely used in aircraft structures, such as AA2024-T3, are extremely susceptible to localized corrosion. For instance, any predictive model for corrosion must be based on realistic data on the propagation kinetics of localized corrosion. Unfortunately, there are currently no standard methods for quantitative measurement of localized corrosion kinetics. Many assumptions regarding the number and morphology of pits are needed to translate measured current transients into pit growth rate. Pit growth kinetics also have been evaluated optically using a microscope to focus on the bottom of the pit, and thereby determining pit depth.[1] Clearly, this method is only accurate when the pit bottom is visible from the top. However, X-ray microfocal radiography showed that pits in thin AA2024-T3 can take circuitous paths as they grow so that much of the pit is not visible from above.[2] Furthermore, pits have been shown to develop into other forms of localized corrosion, such as exfoliation or intergranular corrosion (IGC).[3,4] The growth kinetics of various forms of localized corrosion can surely vary. Few reports of quantitative measurements of the kinetics of IGC in Al alloys exist,[4,5] and little is known about the influence of alloy microstructure on localized corrosion kinetics. In this work, the foil penetration technique and metallographic cross sections were used to address localized corrosion kinetics and morphology in AA2024-T3 in different orientations relative to the rolling direction.

The foil penetration technique was developed by Hunkeler and Bohni.[6] One side of a thin foil is exposed to the solution either at open circuit or under potential control. A detector on the foil back side allows for determination of the time for the fastest-growing site of attack, be it a

pit or IGC, to penetrate a foil of a given thickness. By measuring the penetration time for different foil thicknesses, the penetration depth as a function of time is determined.

Experimental

Longitudinal (L), long transverse (LT), and short transverse (ST) foil sections with different thicknesses were cut from a 1.95 cm thick AA2024-T3 plate along the three alloy directions using a band saw or electric discharge machining (EDM). The convention utilized for the various sections is given in Fig. 1, along with the microstructure of the plate. The ST direction is the through-thickness direction in the rolled plate, and the L direction is along the rolling direction. The sections are labeled according to the perpendicular direction. The samples were ground and polished to 800 grit on both sides with methanol or Beuhler extender. Such nonaqueous polishing minimized corrosion during sample preparation. All samples were degreased with ethanol before attachment to the bottom of an acrylic cell.

Anodic potentiodynamic polarization experiments were performed in deaerated 1 M NaCl to determine the pitting potential of AA2024-T3 as a function of surface orientation relative to the rolling direction. The solution was deaerated by Ar for at least 24 h before the polarization experiment and was continuously purged with Ar during the measurement. Each sample was exposed to the solution for 35 min prior to the start of the measurement. The pitting potential was taken as the point in the anodic polarization curve at which the current increased sharply.

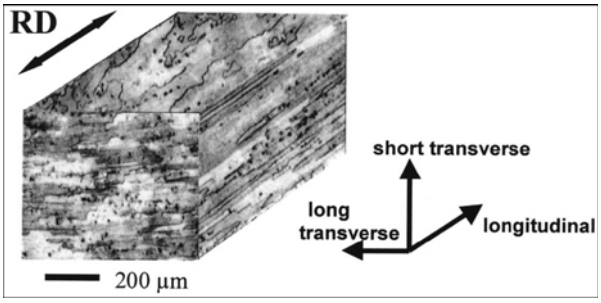

Figure 1. Metallographic sections of AA2024-T3. Also given is the Terminology used for the different sections.

A Teflon knife-edge O-ring exposed an area of 1 cm^2 for the foil penetration experiments. Prior to the start of each penetration experiment, the samples were activated at -0.29 mV saturated calomel electrode (SCE) for 1 s to initiate pits. The sample potential was then stepped immediately to a given value. Details of the procedure used and the detection system can be found elsewhere.[2]

Some samples were metallographically cross-sectioned after the penetration experiments to determine the localized corrosion growth paths and morphology through the foil thickness. The cross sections were examined in the as-polished condition, *i.e.*, without etching.

Results and Discussion

Table I shows the influence of sample orientation on the pitting potential in 1 M NaCl determined by potentiodynamic polarization at a 0.1 mV/s scan rate. The reported values are the average of at least three separate experiments and the standard deviations were about 15 mV. The pitting potential of AA2024-T3 was almost independent of the sample orientation relative to

the rolling direction. Measurements made at a scan rate of 0.5 mV/s exhibited almost identical breakdown values.

Table I. Pitting potentials of AA2024-T3 sections in deaerated 1 M NaCl at a scan rate of 0.1 mV/s.

Sample orientation	E_{pit} (mV SCE)	
	Average	Standard deviation
ST	-668	17
L	-667	11
LT	-661	16

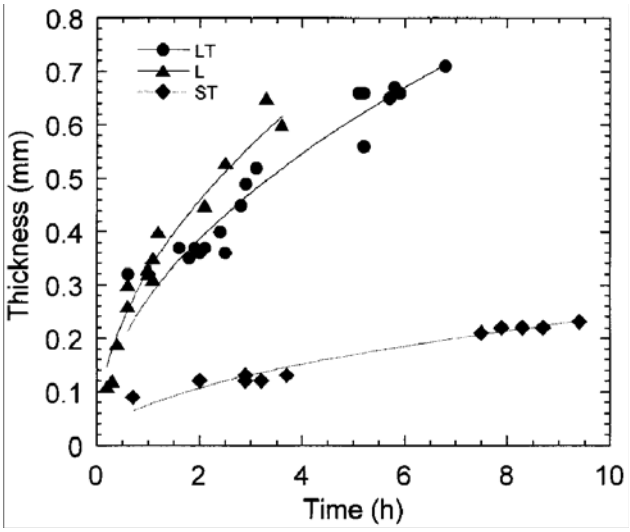

Figure 2. Penetration time for AA2024-T3 foils of varying thickness at -580 mV SCE in O2 bubbled 1.0 M NaCl. Data are plotted as thickness as a function of time to represent the growth kinetics of the fastest-growing corrosion site.

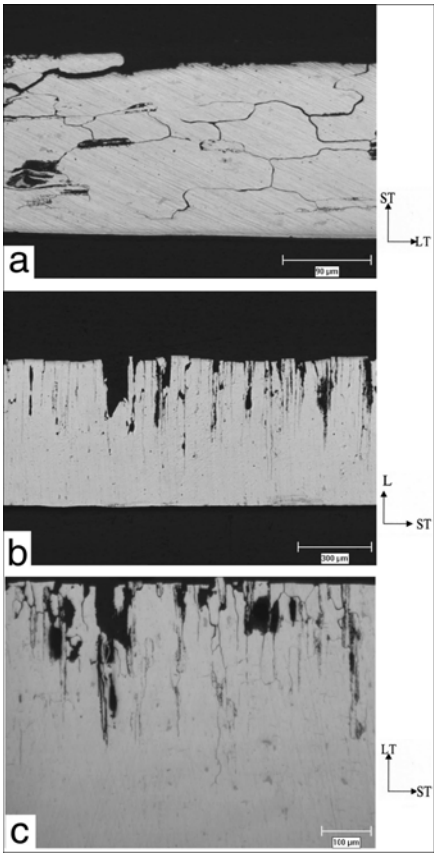

Figure 3. Metallographic cross sections of penetrated thin film samples of varying orientation (a) ST, (b) L, and (c) LT.

Figure 2 shows foil penetration results for ST, L, and LT sections exposed to O2 bubbled 1.0 M NaCl at a controlled potential of -580 mV SCE. The experiments generated penetration times for foils of varying thickness, but the data are plotted as the thickness (or depth of the fastest-growing localized corrosion site) as a function of time. It is clear that the kinetics of localized corrosion growth in AA2024-T3 plate exhibit a strong anisotropy. Growth in the longitudinal direction was slightly faster than that in the long transverse direction, and much faster than that in the short transverse direction. This anisotropic growth behavior can be attributed to the alloy microstructure anisotropy, Fig. 1, and is indirect evidence that the path of attack in this material under these conditions is intergranular. In other words, the pits that initiated on the surface of the AA2024-T3 sections transformed into IGC as they grew. The growth of IGC through ST sections must take circuitous paths because of the alignment of the grains. This is supported by the previously published X-ray radiographic evidence.[2] In contrast, IGC growth in both L and LT directions can take relatively straight paths, so the net growth kinetics are faster. Even if the local IGC growth velocity is identical for the various orientations, the IG path length through the foils is different because of the aspect ratios of the grains.

Direct evidence for the association of localized corrosion growth pathways with grain boundaries was obtained by metallographic cross sections. Figure 3a-c shows cross sections of

ST, L, and LT samples held at -580 mV SCE in oxygenated 1 M NaCl. Recall that the designation of ST, L, or LT describes the through-thickness direction of each foil. Both pitting and IGC can be seen. Transition of pits to IGC is evident. Considerable IG attack occurring on L and LT samples may be rationalized in terms of both availability and susceptibility of grain boundaries. It can be seen that IGC in both the L and LT directions may originate directly from the exposed surface along elongated grain boundaries, which creates a fast penetration path through the foil. Interestingly, as mentioned above, the pitting potential of A2024-T3 does not vary significantly with direction relative to the rolling direction. So pitting potentials provide no information on growth kinetics for AA2024-T3.

Pit growth kinetics have been shown to follow the equation

$$d_p = at^n \quad [1]$$

where d_p is the pit depth, t is time, and a and n are constants dependent on the metal and environment.[7] The value of n has been found to be close to 0.5 for pits in pure Al.[6-8] The $t^{1/2}$ dependence of pit growth has also been modeled by several authors.[9-11] Interestingly, the data from this study, which primarily describe IGC kinetics, can also be well described by $d = at^{1/2}$. The lines in Fig. 2 are fit to this equation; the values of a determined from the fits are 0.0756 (R^2 = 0.98), 0.2733 (R^2 = 0.96), and 0.3244 (R^2 = 0.97), for the ST, LT, and L sections, respectively. These values, and the relative kinetics of localized corrosion, probably depend on the aspect ratios of the grains, which, in turn, can depend on the extent of reduction from the cast ingot. The anisotropy of growth kinetics may be different for a thin sheet.

The idea of the existence of a preferential anodic path as a result of solute enrichment in grain boundary regions is well known.[12] However, it is not clear what makes the grain boundary so susceptible in AA2024-T3 under these conditions, *i.e.*, whether it is the precipitation of intermetallic particles in the grain boundary or the copper-depleted zone along the grain boundary or their combination or the grain boundary properties. Further work is underway to understand IGC susceptibility and influence of anodic potentials, overaging, and environment conditions on IGC growth kinetics.

Conclusions

The growth kinetics of localized corrosion in AA2024-T3 were investigated by the foil penetration technique. The growth in the ST direction was much slower than that in either L or LT direction. Metallographic cross sections confirmed that the difference was a result of the microstructural anisotropy. Pits initiated on the surface transformed into intergranular corrosion, and the intergranular path length was strongly dependent on orientation. In contrast, the pitting potential of AA2024-T3 was almost independent of sample orientation relative to the rolling direction.

Acknowledgments

This work was supported by the United States Air Force Office of Scientific Research through grant no. F49620-99-1-0103.

The Ohio State University assisted in meeting the publication costs of this article.

* Electrochemical Society Student Member.
** Electrochemical Society Active Member.
[z] E-mail: frankel.10@osu.edu

References

1. W. K. Cheung, P. E. Francis, and A. Turnbull, *Mater. Sci. Forum*, **192-194**, 185 (1995).
2. A. Sehgal, G. S. Frankel, B. Zoofan, and S. Rokhlin, *J. Electrochem. Soc.*, **147**, 140 (2000).
3. V. Guillaumin and G. Mankowski, *Corros. Sci.*, **41**, 421(1999).
4. V. Guillaumin and G. Mankowski, in *Critical Factors in Localized Corrosion III*, P. M. Natishan, R. G. Kelly, G. S. Frankel, and R. C. Newman, Editors, PV 98-17, p. 203, The Electrochemical Society Proceedings Series, Pennington, NJ (1999).
5. A. Rota and H. Bohni, *Werkt. Korros.*, **40**, 219 (1989).
6. F. Hunkeler and H. Bohni, *Corrosion*, **37**, 645 (1981).
7. F. Hunkeler and H. Bohni, *Corrosion*, **40**, 535 (1984).
8. F. Hunkeler and H. Bohni, in *Corrosion Chemistry within Pits, Crevices and Cracks*, A. Turnbull, Editor, p. 27, HMSO Books, London (1987).
9. J. W. Tester and H. S. Isaacs, *J. Electrochem. Soc.*, **122**, 1438 (1975).
10. H.H. Strehblow, *Werkst. Korros.*, **35**, 437 (1984).
11. T. R. Beck and R. C. Alkire, *J. Electrochem. Soc.*, **126**, 1662 (1979).
12. J. R. Galvele and S. M. De Micheli, *Corros. Sci.*, **10**, 795 (1970).